Electronic Supplementary Material (ESI) for Dalton Transactions.

Supporting Information

for

Gradual Solid State Redox-Isomerism in the Lanthanide Series

Daria A. Lukina,[a] Alexandra A. Skatova,[a] Roman V. Rumyantcev,[a] Serhiy V. Demeshko,[b] Franc Meyer[b] and Igor L. Fedushkin[a*]

[a] *G.A. Razuvaev Institute of Organometallic Chemistry of Russian Academy of Sciences, Tropinina 49, Nizhny Novgorod 603950, Russian Federation*

[b] *Institut für Anorganische Chemie, Universität Göttingen, Tammannstrasse 4, 37077 Göttingen, Germany*

Contents

UV-vis spectrum

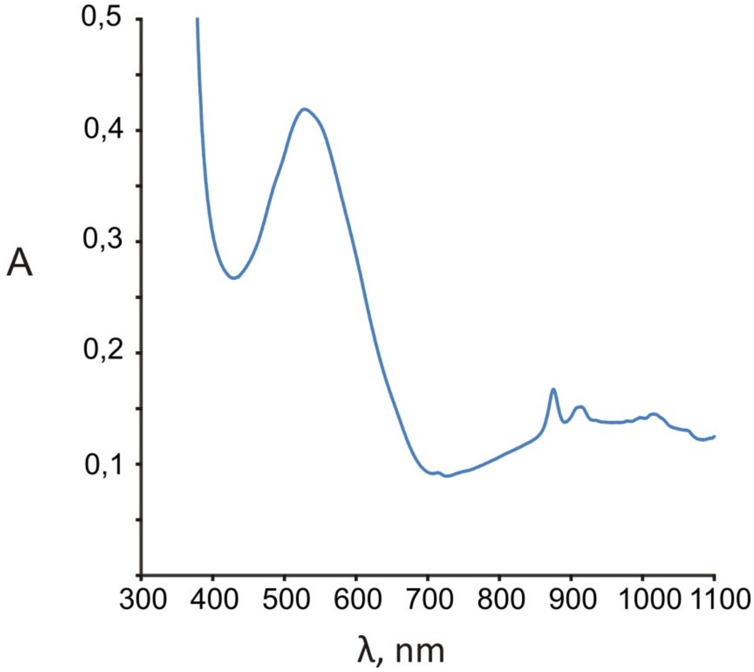

Fig. 1S. UV/Vis spectrum of [(Ar^{BIG}-bian)YbCl]$_2$ in toluene (10^{-4} mol/L) in the Pyrex cell (3.5 mm).

NMR spectrum

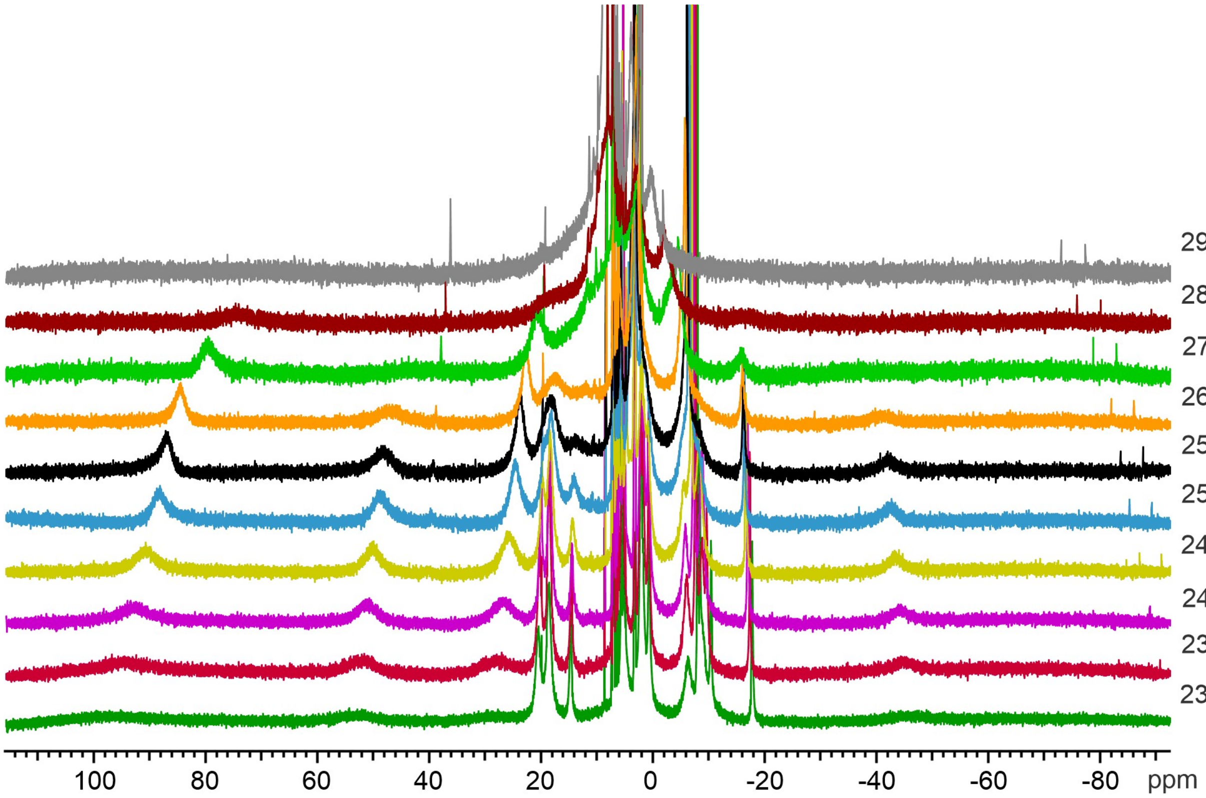

Fig. 2S. Temperature dependence of the ^{1}H NMR spectrum of **2** (400 MHz, toluene-d$_8$).

IR spectrum

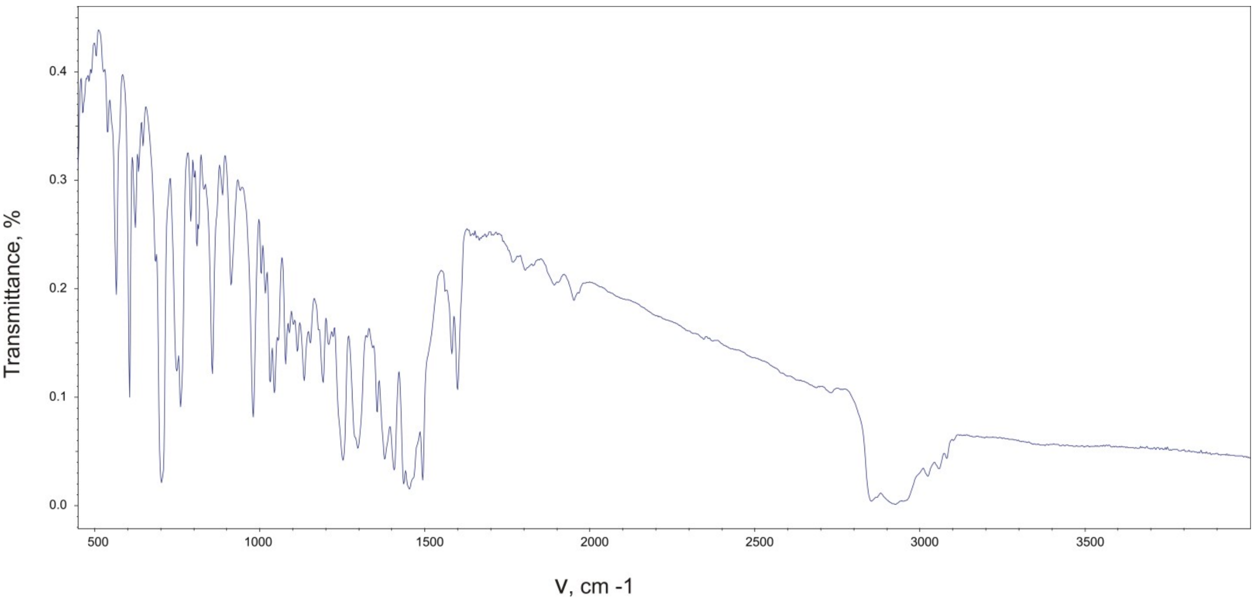

Fig. 3S. IR spectrum of **2** in the solid state.

X-ray crystallography

The X-ray diffraction data for complex **2** were collected on Bruker AXS SMART APEX equipped with a low-temperature Helix attachment (Oxford Cryosystems) (40 K) and Bruker D8 Quest Photon II (100, 190 and 350 K) diffractometers (Mo-Kα radiation, ω-scan technique, λ = 0.71073 Å). The intensity data were integrated by SAINT program [1]. Absorption corrections for **2** were performed using the SADABS program [2]. The structures were solved by direct (40 K) and dual method [3] (100, 190 and 350 K) and refined on F_{hkl}^2 using SHELXTL package [4]. All non-hydrogen atoms were refined anisotropically. All hydrogen atoms were placed in calculated positions and were refined in the riding model ($U_{iso}(H) = 1.5U_{eq}(C)$ for CH_3-groups and $U_{iso}(H) = 1.2U_{eq}(C)$ for other groups). The twinning matrix [-1 0 0 0 0 -1 0 -1 0] was used at 100 K and the refinement resulted in a twin fraction of 0.36. The presence of twinning at 100 K is due to the close values of the *b* and *c* axes as well as the α and β angles. There are problems with refining the geometry and thermal parameters of the organic part of complex **2** at 40 K. In addition, disorder of some phenyl substituents and DME molecules is observed at 190 and 350 K. The instructions SADI, DFIX, AFIX 66, EADP and ISOR were imposed to maintain reasonable geometries and adequate thermal ellipsoids of carbon, nitrogen and oxygen atoms in disordered fragments at 190 and 350 K and organic part at 40 K.

The main crystallographic data and structure refinement details for complex **2** are presented in Table 1S. The crystallographic data have been deposed in the Cambridge Crystallographic Data Centre under the deposition codes CCDC 2278220 (40 K), 2278221 (100 K), 2278222 (190 K) and 2278223 (350 K). These data can also be obtained free of charge at ccdc.cam.ac.uk/structures/ from the Cambridge Crystallographic Data Centre.

Table 1S. The main crystallographic data and structure refinement details for compound **2**.

Complex	**2**			
Temperature/K	40(2)	100(2)	190(2)	350(2)
Formula	$C_{85}H_{76}N_3O_2S_2Yb$			
Formula weight	1408.64			
Crystal system	Triclinic	Triclinic	Monoclinic	Monoclinic
Space group	*P–1*	*P–1*	$P2_1/n$	$P2_1/n$
a/Å	13.5146(8)	13.5191(5)	13.5724(6)	13.6757(5)
b/Å	32.1214(18)	32.1317(12)	25.3618(11)	25.5176(9)
c/Å	32.1214(18)	32.1481(12)	59.899(3)	20.2107(7)
α/deg	103.63(1)	103.6396(12)	90	90
β/deg	90.853(3)	90.8641(13)	91.2838(14)	91.5527(11)
γ/deg	90.853(3)	90.8324(13)	90	90
V/Å^3	13547.3(13)	13567.1(9)	20613.2(15)	7050.4(4)
Z	8	8	12	4
density/g/sm^3	1.381	1.379	1.362	1.327
μ/mm^{-1}	1.495	1.493	1.474	1.436
F(000)	5800	5800	8700	2900
Crystal size/mm	0.32×0.26×0.18	0.31×0.29×0.26		
θ-range/deg	2.009-28.410	0.652-29.575	1.880-29.575	2.168-29.574
Index ranges	$-17 \le h \le 17$	$-18 \le h \le 18$	$-18 \le h \le 18$	$-18 \le h \le 18$
	$-42 \le k \le 42$	$-43 \le k \le 44$	$-35 \le k \le 34$	$-35 \le k \le 35$
	$-42 \le l \le 42$	$-44 \le l \le 44$	$-83 \le l \le 83$	$-28 \le l \le 28$
Reflections collected/unique	107477 / 65447	233552 / 76047	341308 / 57738	118301 / 19758
R_{int}	0.1272	0.0488	0.0490	0.0282
Data/restraints/ parameters	65447 / 2175 / 2947	76047 / 0 / 3374	57738 / 35 / 2559	19758 / 533 / 871
S	0.800	1.017	1.065	1.036
R_1/wR_2 (I>2σ(I))	0.0593 / 0.0897	0.0321 / 0.0624	0.0493 / 0.1207	0.0373 / 0.0827
R_1/wR_2 (all parameters)	0.1291 / 0.1102	0.0391 / 0.0643	0.0664 / 0.1277	0.0553 / 0.0905
Largest diff peak/hole [e Å^{-3}]	2.204/–1.930	1.032/–1.644	1.825/–2.023	0.707/–0.886

Table 2S. Selected bond lengths [Å] and angles [°] in compound **2** at 40 K.

Bond / Angle	**A^{40} (2b)**	**B^{40} (2a)**	**C^{40} (2a)**	**D^{40} (2a)**	**$B^{40}C^{40}D^{40}$ averaged**
Yb(1)–N(1)	2.462(5)	2.217(5)	2.228(5)	2.216(5)	2.220
Yb(1)–N(2)	2.431(4)	2.214(4)	2.187(4)	2.205(4)	2.202
Yb(1)–O(1)	2.453(4)	2.382(4)	2.358(4)	2.381(4)	2.374
Yb(1)–O(2)	2.505(4)	2.391(4)	2.365(4)	2.374(4)	2.377
Yb(1)–S(1)	2.8720(16)	2.7989(16)	2.7814(16)	2.7818(16)	2.787
Yb(1)–S(2)	2.8195(16)	2.7057(16)	2.6904(16)	2.6787(16)	2.692
C(1)–N(1)	1.331(6)	1.421(6)	1.413(6)	1.413(6)	1.416
C(2)–N(2)	1.352(7)	1.410(7)	1.419(7)	1.421(7)	1.417
C(1)–C(2)	1.455(7)	1.394(7)	1.388(7)	1.399(7)	1.394
S(1)–C(79)	1.727(6)	1.723(6)	1.713(6)	1.734(6)	1.723
S(2)–C(79)	1.717(6)	1.734(6)	1.750(6)	1.709(6)	1.731
N(2)–Yb(1)–N(1)	71.40(15)	80.18(17)	81.41(16)	80.23(17)	80.61
O(1)–Yb(1)–O(2)	67.95(12)	68.24(13)	69.49(13)	68.42(12)	68.72
S(2)–Yb(1)–S(1)	63.09(4)	65.04(5)	65.78(5)	65.60(5)	65.47
N(2)–Yb(1)–S(2)	98.94(11)	96.27(12)	101.97(12)	105.14(13)	101.13
N(1)–Yb(1)–S(2)	98.65(11)	98.94(13)	98.78(12)	94.26(12)	97.33
N(2)–Yb(1)–S(1)	135.61(12)	130.28(12)	110.98(12)	116.12(13)	119.13
N(1)–Yb(1)–S(1)	146.75(10)	144.93(12)	161.42(12)	156.17(11)	154.17

Table 3S. The root-mean-square deviations of atomic positions of independent molecules of compound **2** at 40 K.

Molecule	**A^{40}**	**B^{40}**	**C^{40}**	**D^{40}**
A^{40}	-	0.7203	0.5753	0.8674
B^{40}	0.7203	-	0.5630	0.4537
C^{40}	0.5753	0.5630	-	0.5343
D^{40}	0.8674	0.4537	0.5343	-

Table 4S. Selected bond lengths [Å] and angles [°] in compound **2** at 100 K.

Bond / Angle	**A^{100}**	**B^{100}**	**C^{100}**	**D^{100}**	**B^{100}C^{100}D^{100} averaged***
Yb(1)–N(1)	2.452(2)	2.230(2)	2.213(2)	2.220(2)	2.221
Yb(1)–N(2)	2.430(2)	2.193(2)	2.211(2)	2.211(2)	2.205
Yb(1)–O(1)	2.444(2)	2.3642(19)	2.373(2)	2.3917(19)	2.376
Yb(1)–O(2)	2.5044(19)	2.364(2)	2.3688(19)	2.3941(19)	2.376
Yb(1)–S(1)	2.8721(8)	2.7765(7)	2.7756(8)	2.7933(7)	2.782
Yb(1)–S(2)	2.8238(8)	2.6851(7)	2.6824(8)	2.7047(7)	2.691
C(1)–N(1)	1.336(3)	1.411(3)	1.407(3)	1.398(3)	1.405
C(2)–N(2)	1.336(3)	1.407(3)	1.405(3)	1.406(3)	1.406
C(1)–C(2)	1.454(3)	1.391(3)	1.383(4)	1.388(3)	1.387
S(1)–C(79)	1.728(3)	1.722(3)	1.728(3)	1.729(3)	1.726
S(2)–C(79)	1.718(3)	1.726(3)	1.716(3)	1.711(3)	1.718
N(2)–Yb(1)–N(1)	71.53(7)	81.00(8)	80.11(8)	80.02(7)	80.38
O(1)–Yb(1)–O(2)	67.96(7)	69.42(7)	68.61(7)	68.41(7)	68.81
S(2)–Yb(1)–S(1)	63.02(2)	65.62(2)	65.46(2)	64.77(2)	65.28
N(2)–Yb(1)–S(2)	98.96(6)	102.53(6)	104.74(6)	97.21(6)	101.49
N(1)–Yb(1)–S(2)	98.35(6)	98.97(6)	94.13(6)	98.41(6)	97.17
N(2)–Yb(1)–S(1)	135.55(6)	112.46(6)	117.26(6)	129.36(6)	119.69
N(1)–Yb(1)–S(1)	146.49(5)	160.86(6)	155.29(6)	145.84(6)	154.00

* - **B^{100}C^{100}D^{100}$_{\mathbf{average}}$** =

$$\frac{(Bond/Angle\ in\ molecule\ B) + (Bond/Angle\ in\ molecule\ C) + (Bond/Angle\ in\ molecule\ D)}{3}$$

Table 5S. Selected bond lengths [Å] and angles [°] in compound **2** at 190 K.

Bond / Angle	**A^{190}**	**B^{190}**	**C^{190}**	**B^{190}C^{190} averaged**
Yb(1)–N(1)	2.422(3)	2.222(3)	2.198(3)	2.210
Yb(1)–N(2)	2.405(3)	2.242(3)	2.215(3)	2.229
Yb(1)–O(1)	2.425(3)	2.400(3)	2.360(3)	2.380
Yb(1)–O(2)	2.493(3)	2.375(3)	2.370(2)	2.373
Yb(1)–S(1)	2.8032(10)	2.7822(11)	2.7772(9)	2.780
Yb(1)–S(2)	2.8726(11)	2.7037(11)	2.6830(9)	2.693
C(1)–N(1)	1.344(4)	1.401(4)	1.407(4)	1.404
C(2)–N(2)	1.343(4)	1.388(4)	1.404(4)	1.396
C(1)–C(2)	1.445(4)	1.403(4)	1.398(4)	1.401
S(1)–C(79)	1.718(4)	1.709(4)	1.716(4)	1.713
S(2)–C(79)	1.719(4)	1.713(4)	1.725(4)	1.719
N(2)–Yb(1)–N(1)	72.65(9)	79.14(9)	80.70(9)	79.93
O(1)–Yb(1)–O(2)	67.82(10)	68.02(10)	68.81(9)	68.42
S(2)–Yb(1)–S(1)	63.10(3)	64.45(3)	65.58(3)	65.02
N(2)–Yb(1)–S(2)	134.92(7)	97.11(7)	96.56(7)	96.84
N(1)–Yb(1)–S(2)	145.28(7)	100.45(7)	104.83(7)	102.64
N(2)–Yb(1)–S(1)	98.84(7)	151.38(7)	158.24(7)	154.81
N(1)–Yb(1)–S(1)	96.60(7)	123.91(7)	114.82(7)	119.37

Table 6S. The root-mean-square deviations of atomic positions of independent molecules of compound **2** at 190 K.

Molecule	**A^{190}**	**B^{190}**	**C^{190}**
A^{190}	-	0.6361	0.7259
B^{190}	0.6361	-	0.3108
C^{190}	0.7259	0.3108	-

Table 7S. Selected bond lengths [Å] and angles [°] in compound **2** at 350 K.

E^{350}			
Bond		**Bond**	
Yb(1)–N(1)	2.3460(19)	Yb(1)–N(2)	2.3242(19)
Yb(1)–O(1)	2.404(2)	Yb(1)–O(2)	2.439(2)
Yb(1)–S(1)	2.8285(10)	Yb(1)–S(2)	2.7500(10)
C(1)–N(1)	1.362(3)	C(2)–N(2)	1.367(3)
S(1)–C(79)	1.708(3)	S(2)–C(79)	1.702(3)
C(1)–C(2)	1.424(3)		
Angle		**Angle**	
N(1)–Yb(1)–N(2)	75.50(6)	O(1)–Yb(1)–O(2)	67.97(8)
N(1)–Yb(1)–S(1)	150.66(5)	N(2)–Yb(1)–S(1)	126.74(5)
N(1)–Yb(1)–S(2)	96.16(5)	N(2)–Yb(1)–S(2)	100.89(5)
S(1)–Yb(1)–S(2)	63.46(3)		

Table 8S. SHAPE analysis for compound **2**.

T, K	Molecule	**JPPY-6**	**TPR-6**	**OC-6**	**PPY-6**	**HP-6**
40	**A**	17.691	2.633	15.555	14.795	28.798
	B	19.099	2.145	14.222	15.878	29.200
	C	20.115	7.260	5.716	17.054	30.213
	D	18.088	6.121	7.112	15.033	31.386
100	**A**	17.624	2.638	15.504	14.755	28.767
	B	19.838	6.986	5.982	16.782	30.229
	C	17.896	5.745	7.493	14.843	31.487
	D	18.787	2.250	13.723	15.573	29.385
190	**A**	17.427	2.511	15.490	14.591	27.658
	B	17.812	3.347	11.148	14.663	30.043
	C	18.886	6.846	6.500	15.882	31.234
350	**E**	17.162	3.329	11.689	14.162	29.798
JPPY-6: Johnson pentagonal pyramid J2 TPR-6: Trigonal prism OC-6: Octahedron PPY-6: Pentagonal pyramid HP-6: Hexagon [5]						

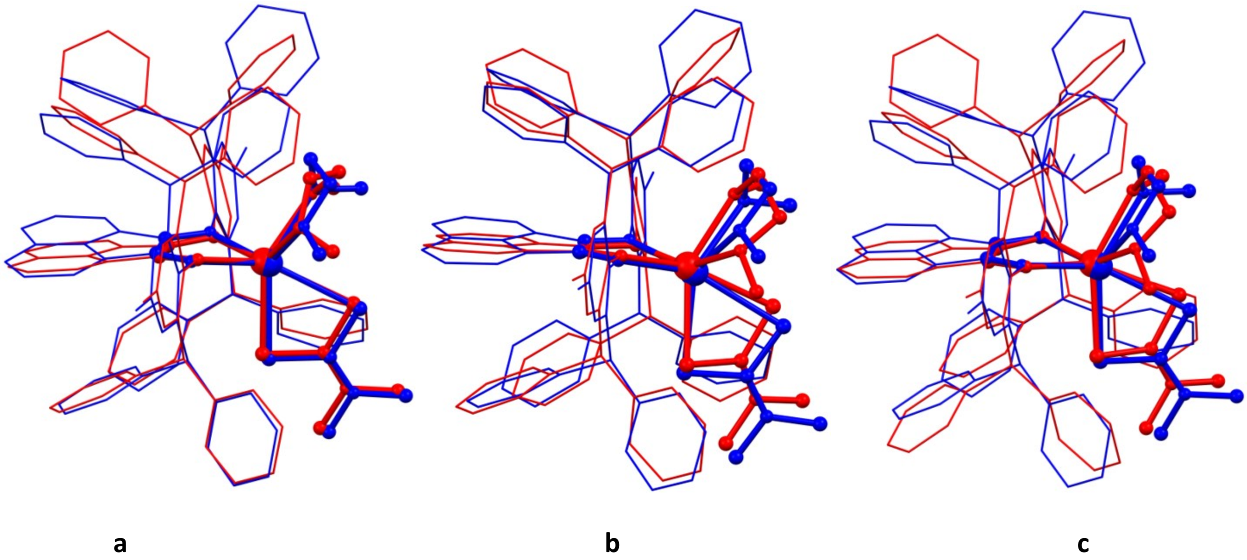

Figure 4S. Overlay of molecules **A**^{40} (blue) and **B**^{40} (red) (**a**), **A**^{40} (blue) and **C**^{40} (red) (**b**), **A**^{40} (blue) and **D**^{40} (red) (**c**).

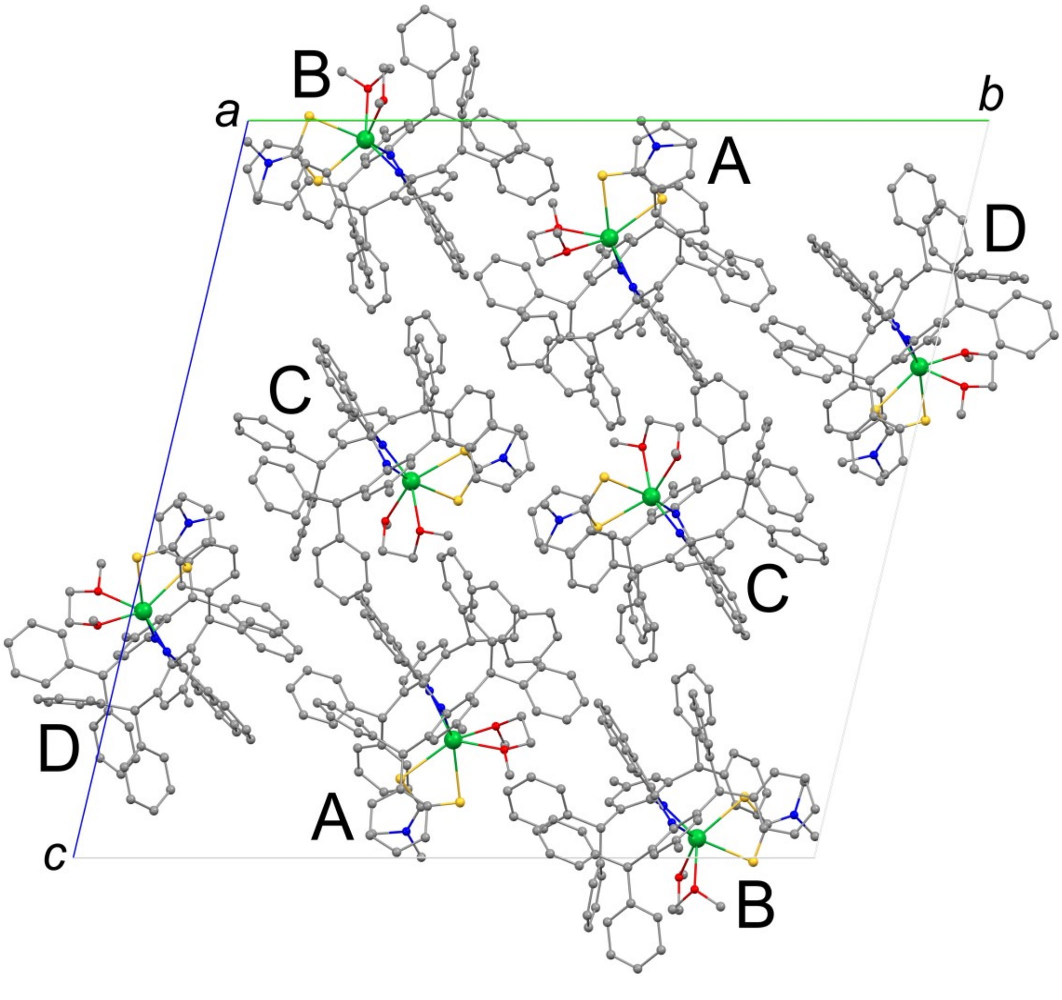

Fig. 5S. Fragment of the crystal packing of complex **2** at 40 K.

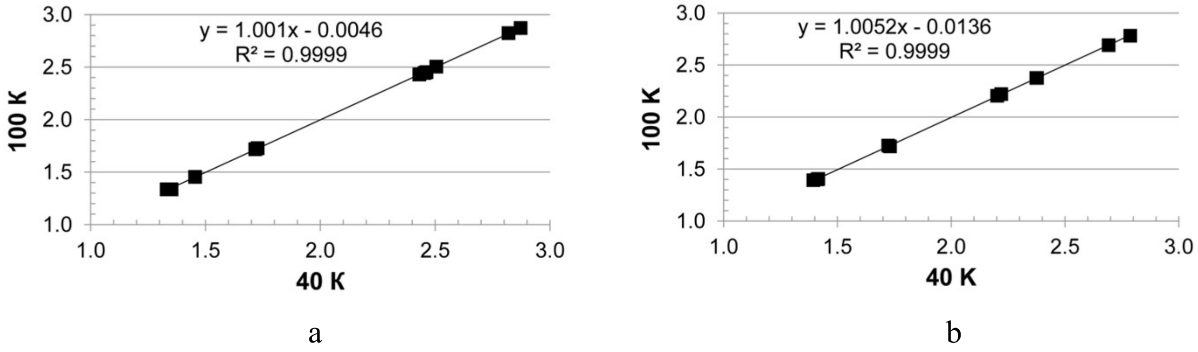

Fig. 6S. The linear correlation diagrams for selected bond lengths in molecule **A** (a) and corresponding averaged values in molecules **B**, **C** and **D** (b) at 40 and 100 K.

The root-mean-square deviation of atomic positions (RMSD) for 12 molecules without hydrogen atoms and phenyl substituents at 40 and 100 K is 0.031 Å :

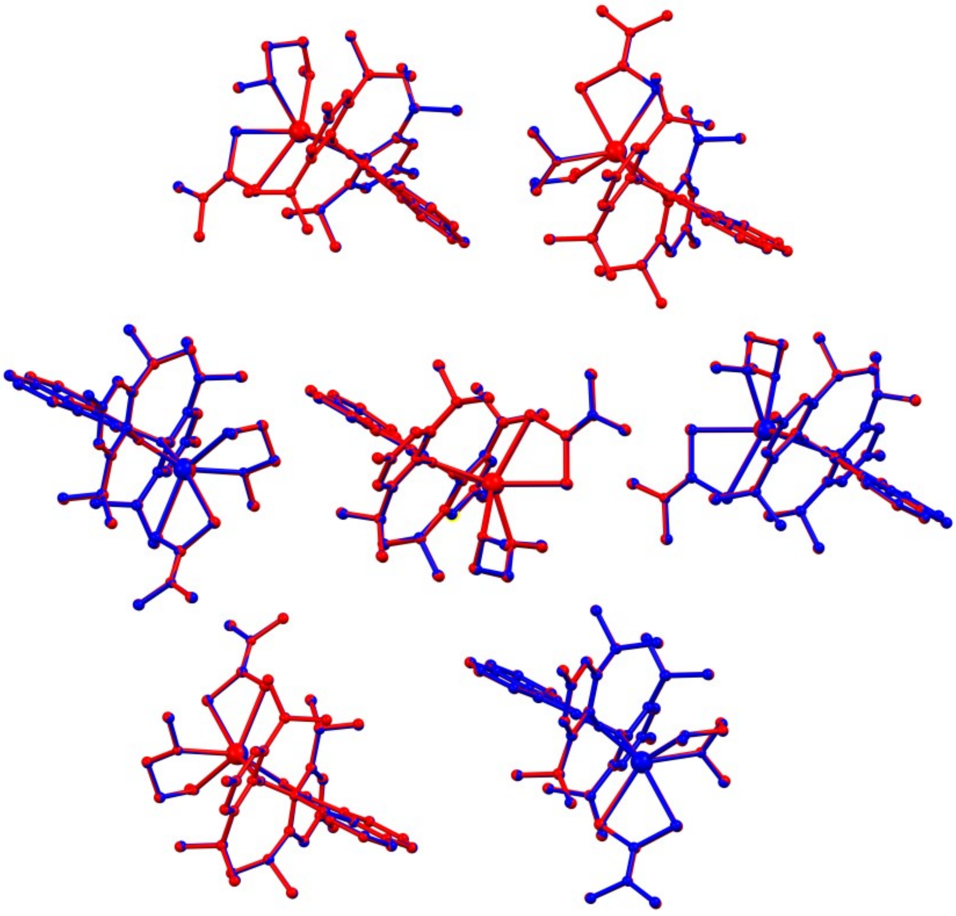

Fig. 7S. Comparison of the crystal structure at 40 K (red) and 100 K (blue) of compound **2**. Hydrogen atoms and phenyl substituents are omitted for clarity.

Similar to lower temperatures, the greatest root-mean-square deviations of atomic positions is observed when comparing molecules $\mathbf{A^{190}}\leftrightarrow\mathbf{B^{190}}$ and $\mathbf{A^{190}}\leftrightarrow\mathbf{C^{190}}$ (Table 6S, Fig. 9S). A comparison of the crystal structures at 100 and 190 K of compound **2** is shown in Figure 10S. The RMSD for 12 molecules without hydrogen atoms and phenyl substituents is 0.295 Å.

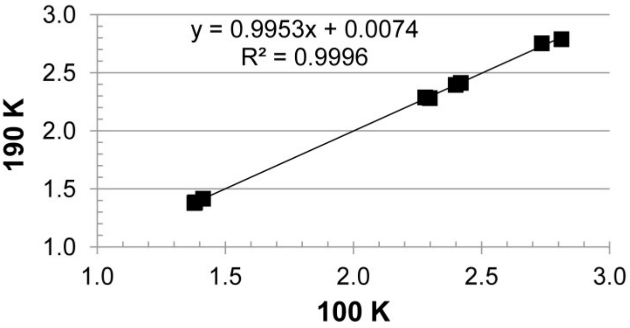

Fig. 8S. The linear correlation diagrams for selected bond lengths that correspond to a 2:1 ratio* at 100 and 190 K.

* - 2:1 ratio at 100 K = $$\frac{2\left(B^{100}C^{100}D^{100}_{average}\right)+\left(Bond\ in\ molecule\ A^{100}\right)}{3};$$

2:1 ratio at 190 K = $$\frac{\left(Bond\ in\ molecule\ A^{190}\right)+\left(Bond\ in\ molecule\ B^{190}\right)+\left(Bond\ in\ molecule\ C^{190}\right)}{3}$$

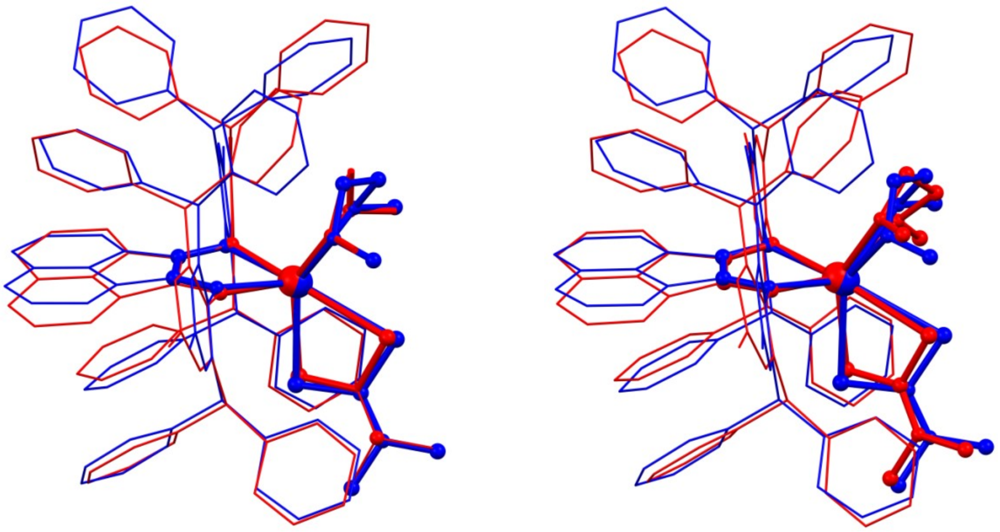

a **b**

Fig. 9S. Overlay of molecules **A**^{190} (blue) and **B**^{190} (red) (**a**) and **A**^{190} (blue) and **C**^{190} (red).

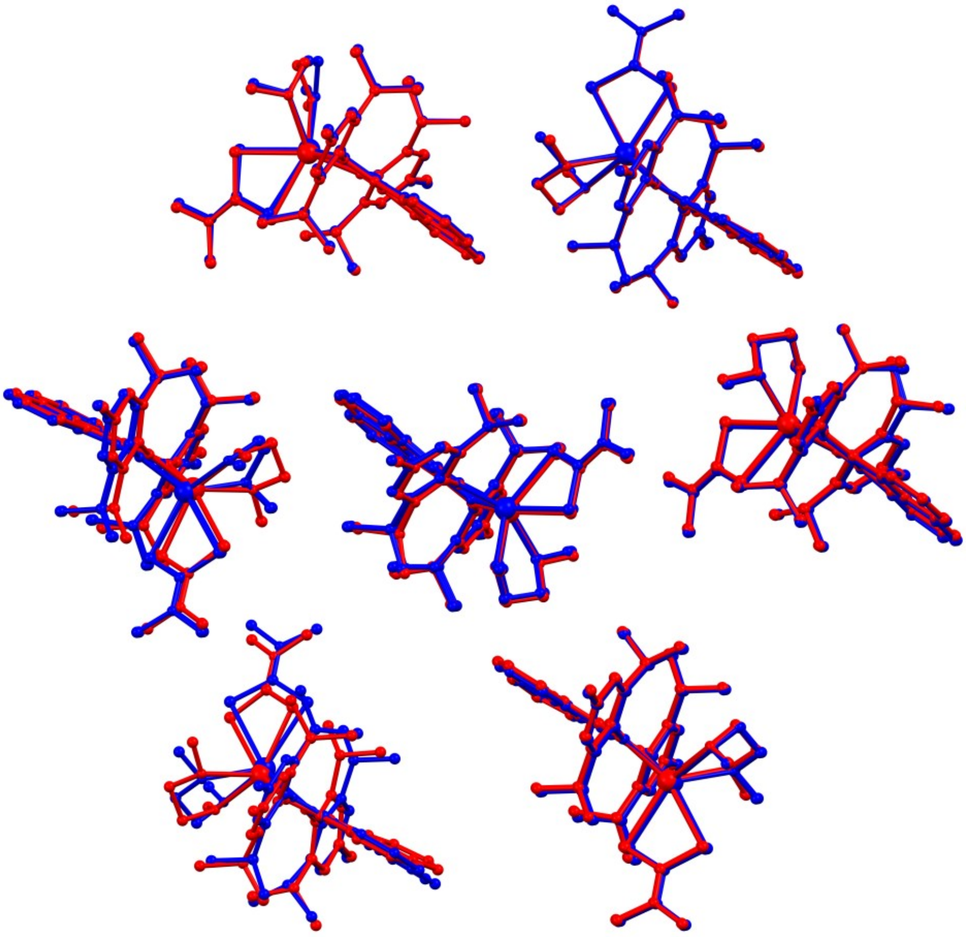

Fig. 10S. Comparison of the crystal structure at 100 K (red) and 190 K (blue) of compound **2**. Hydrogen atoms and phenyl substituents are omitted for clarity.

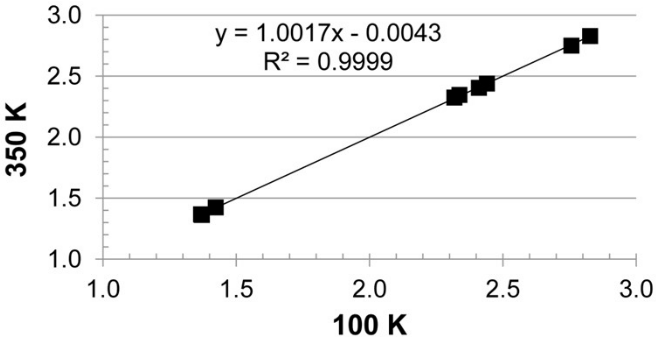

Fig. 11S. The linear correlation diagrams for selected bond lengths that correspond to a 1:1 ratio* at 100 and 350 K.

* - 1:1 ratio at 100 K = $\dfrac{\left(B^{100}C^{100}D_{average}^{100}\right) + \left(Bond\ in\ molecule\ A^{100}\right)}{2}$;

In comparison with the 100 K data, in the crystal measured at 350 K an even stronger divergence of molecules is observed (Fig. 12S). The RMSD for 12 molecules (without hydrogen atoms and phenyl substituents) is 0.428 Å.

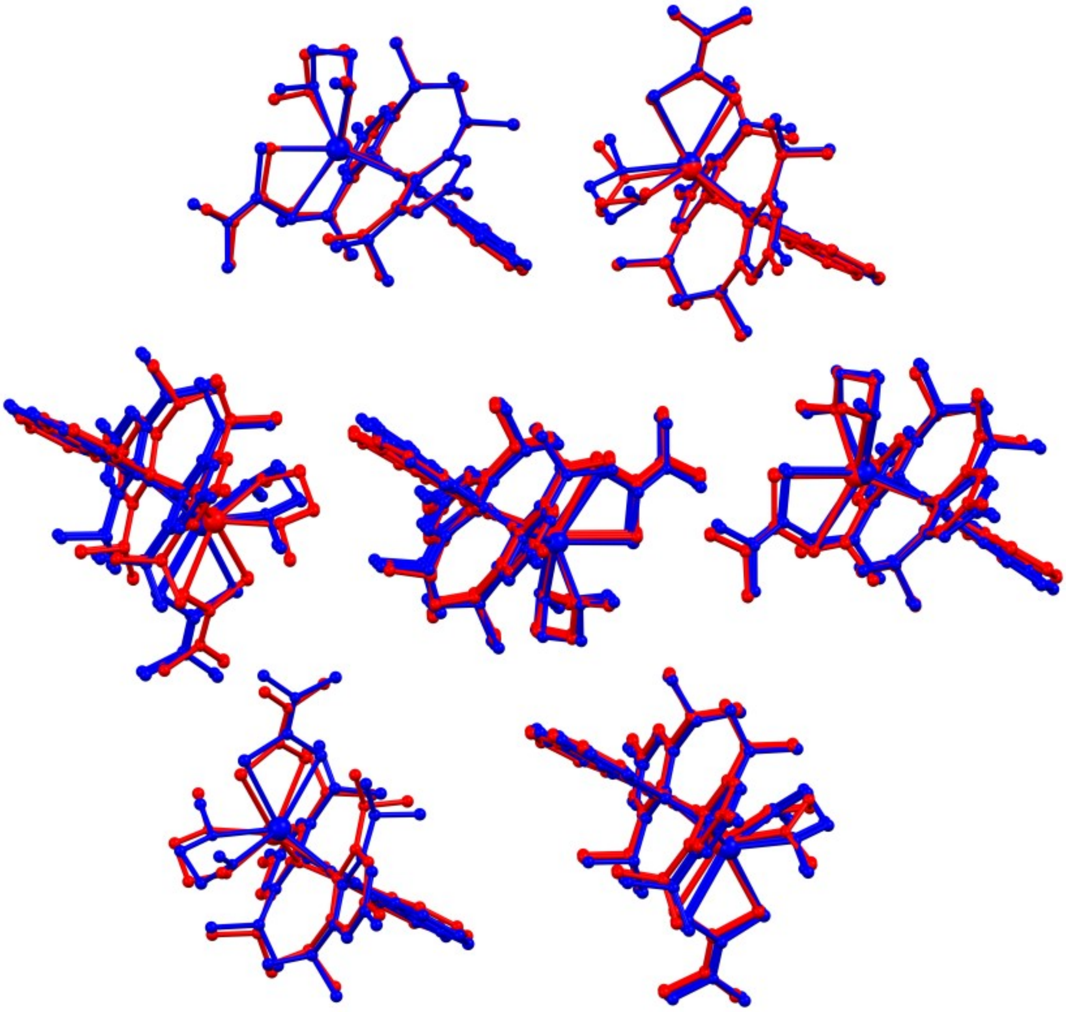

Fig. 12S. Comparison of the crystal structure at 100 K (red) and 350 K (blue) of compound **2**. Hydrogen atoms and phenyl substituents are omitted for clarity.

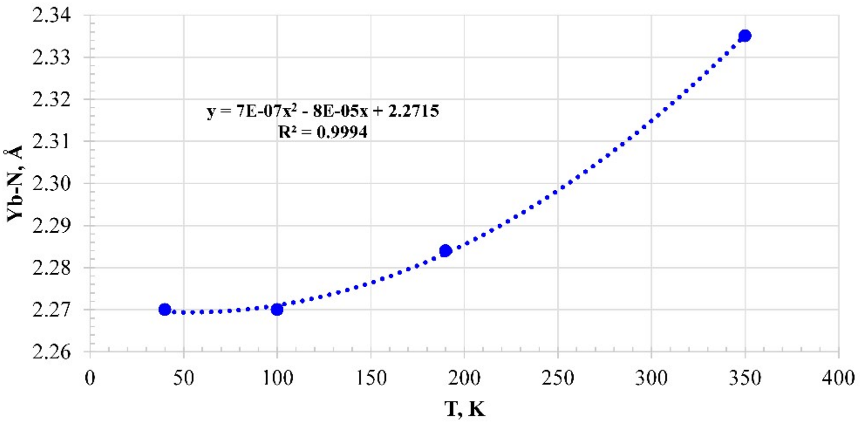

Fig. 13S. Dependence of the average Yb-N bond length in complex **2** on temperature (K).

Magnetic data

Formula 1S. Calculation of the molar fraction of the HT form **2b** [6]:

$$\gamma = \frac{\chi T - (\chi T)_L}{(\chi T)_H - (\chi T)_L}$$

where χT is the the magnetic susceptibility multiplied by temperature of compound **2**;

$(\chi T)_L$ is the magnetic susceptibility multiplied by temperature of the LT isomer **2a** (numerically equal to experimental χT value for [(Ar^{BIG}-bian)YbI(2,2'-bipy)][7]);

$(\chi T)_H$ is the magnetic susceptibility multiplied by temperature of the HT isomer **2b** (0.375 cm^{3}mol^{-1}K) and γ is the molar fraction of the HT isomer **2b**.

The temperature dependence of the magnetic moment of compound **2** in solid state is depicted in Figure 14S. Upon lowering the temperature from 200 to 2 K the magnetic moment is decreasing from 3.5 to 2.8 μ_B. A smooth decrease of the magnetic moment with temperature decreasing is typical for Yb^{3+} derivatives. [8] Together with the X-ray crystallography data the magnetic data point out the presence of isomer **2a** in the crystal of **2**. However, the maximal value of the magnetic moment (3.5 μ_B at 200 K) is noticeably lower than in other Yb^{3+} (electronic configuration [Xe]4f^{13}) species (4.3-4.9 μ_B). [9] This can be explained by the presence of isomer **2b** that contains diamagnetic Yb^{2+} (electronic configuration [Xe]4f^{14}) and the dpp-bian radical-anion (S = ½). Increasing the temperature from 200 to 300 K causes a decrease of the magnetic moment from 3.5 to 3.4 μ_B due to a partial conversion of isomer **2a** into isomer **2b**.

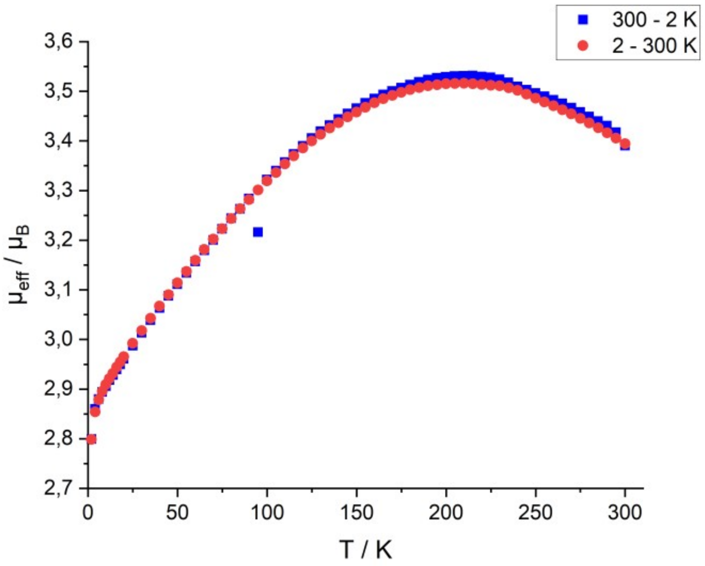

Fig. 14S. The temperature dependence of μeff for compound **2** at 5000 Oe applied magnetic field, recorded in heating (red) and cooling (blue) mode in the indicated temperature range.

References

[1] SAINT, Data Reduction and Correction Program, Bruker AXS, Madison, Wisconsin, USA, 2014.

[2] L. Krause, R. Herbst-Irmer, G.M. Sheldrick, D. Stalke, Comparison of silver and molybdenum microfocus X-ray sources for single-crystal structure determination, *J. Appl. Crystallogr.*, 2015, **48**, 3.

[3] G.M. Sheldrick, SHELXT–Integrated space-group and crystal-structure determination, *Acta Crystallogr., Sect. A: Found. Adv.*, 2015, **71**, 3.

[4] G.M. Sheldrick, Crystal structure refinement with SHELXL, *Acta Crystallogr., Sect. C: Struct. Chem.*, 2015, **71**, 3.

[5]. S. Alvarez, D. Avnir, M. Llunell, M. Pinsky, Continuous symmetry maps and shape classification. The case of six-coordinated metal compounds, *New J. Chem.*, 2002, **26**, 996.

[6] O. Kahn, VCH Publishers Inc., 1993, 380.

[7] V.G. Sokolov, D.A. Lukina, A.A. Skatova, M.V. Moskalev, E.V. Baranov, I.L. Fedushkin, Samarium and ytterbium complexes based on sterically hindered 1,2-bis(imino)acenaphthene, *Russ. Chem. Bull. (Int. Ed.)*, 2021, **70**, 2119.

[8]. L. M. Engelhardt and B. N. Figgis, Magnetic susceptibility of Tm3+ and Yb3+ in cubic NaYF4, J. Chem. Soc. (A): Inor., *Phys. Theor*., 1970, **3**, 415.

[9]. J.-C. Bunzli, Benefiting from the unique properties of lanthanide ions, *G. Acc. Chem. Res.*, 2006, **39**, 53.